# Development and acoustic optimisation of sustainable fibrous materials*

Andrea Santoni[a]* | Francesco Pompoli[a] | Patrizio Fausti[a]

[a] Dipartimento di Ingegneria, Università degli studi di Ferrara, Via Saragat, 1, 44122 Ferrara
* Corresponding author: andrea.santoni@unife.it

**Ricevuto:** 9/9/2025
**Accettato:** 2/10/2025

**DOI:** 10.3280/ria2-2025oa20975
**ISSNe:** 2385-2615

The urgent need for sustainable solutions in different industrial sectors has led to a growing interest in using natural and recycled fibrous materials for acoustic and thermal insulation. While these materials offer significant environmental benefits, their commercial production is still limited also due to a lack of standardised characterization and design methods. This paper addresses this gap by presenting a comprehensive methodology to develop and acoustically optimise sustainable fibrous materials. The approach combines small-scale experimental characterisation with an analytical framework that models acoustic performance as a function of material density. The effectiveness of this method is demonstrated through case studies involving a variety of sustainable materials, including hemp, jute, posidonia, and recycled fibre mixtures. The results validate the methodology's ability to accurately predict the sound-absorbing properties of these materials, enabling the design of high-performance solutions capable of achieving acoustic ratings comparable to traditional materials. This article, invited by the RIA editorial board, is not an original study. Instead, it synthesizes existing research by reanalysing and integrating the data from multiple studies using a single, unified methodology.
**Keywords:** fibrous materials, sustainability, acoustic modelling, JCA, optimisation, sound absorption

**Sviluppo e ottimizzazione acustica di materiali fibrosi sostenibili**
L'impellente necessità di trovare soluzioni sostenibili in diversi settori industriali ha portato a un crescente interesse per l'utilizzo di materiali fibrosi naturali e riciclati per l'isolamento acustico e termico. Sebbene questi materiali offrano significativi vantaggi ambientali, la loro produzione commerciale è ancora limitata anche a causa della mancanza di metodi standardizzati per la loro caratterizzazione e progettazione. Questo articolo affronta tale lacuna presentando una metodologia completa per sviluppare e ottimizzare acusticamente i materiali fibrosi sostenibili. L'approccio integra la caratterizzazione sperimentale su piccola scala con un modello analitico per stimare le prestazioni acustiche di un materiale in funzione della sua densità. L'efficacia di questo metodo è dimostrata attraverso casi di studio che coinvolgono una varietà di materiali sostenibili, tra cui canapa, iuta, posidonia e miscele di fibre riciclate. I risultati validano l'affidabilità della metodologia per la stima delle prestazioni fonoassorbenti di questi materiali, consentendo la progettazione di soluzioni sostenibili in grado di raggiungere prestazioni paragonabili ai materiali tradizionali. Questo articolo, su invito del comitato editoriale RIA, non è uno studio originale. Si tratta invece di una raccolta di ricerche esistenti, i cui dati sono stati rianalizzati e integrati attraverso una metodologia unificata.
**Parole chiave:** materiali fibrosi, sostenibilità, modellazione acustica, JCA, ottimizzazione, assorbimento acustico

## 1 | Introduction

The development of sustainable solutions in various sectors has become a top priority due to global challenges associated with climate change. The construction industry, in particular, is a major contributor to global energy and resource consumption [1-4]. Traditionally, building acoustic and thermal insulation relies on materials derived from petrochemicals, such as polystyrene, or from mineral sources processed with high energy consumption, like mineral wools. While effective, these conventional materials pose significant environmental impacts throughout their life cycle, including the use of non-renewable resources, high embodied energy consumption, and difficulties in recycling and disposal [5, 6]. In alignment with inter-

* Invited paper following the oral presentation at the AIA International Symposium "Innovative Materials in Acoustics: Between Sustainability and Technology" held in Bologna on January 30, 2025.

national imperatives, such as the United Nations Sustainable Development Goals (SDGs), particularly SDG 12 on Responsible Consumption and Production, and the ambitious targets of the European Green Deal, there is an urgent need for innovative solutions that promote resource efficiency and circularity. This has led to a growing interest in the research and development of alternative materials that offer performance comparable to conventional ones but with a significantly reduced environmental footprint. Sustainable fibrous materials for acoustic and thermal applications can be broadly classified into two main categories: natural (bio-based) materials and recycled materials. Natural materials include agricultural and forest by-products, such as hemp, jute, reeds, sugarcane bagasse, straw, and oil palm fibres, which can be processed into panels or loose fibres [7-13]. Recycled materials, on the other hand, originate from industrial and post-consumer waste, such as recycled textile fibres (e.g., cotton, polyester, denim, wool, acrylic) and recycled glass. Their ability to sequester carbon during growth (in the case of bio-based materials) or to reduce landfill waste (for recycled materials) makes them an ideal choice for boosting the circular economy and achieving decarbonization goals. Fibrous (and porous) materials are effective at absorbing sound waves by converting acoustic energy into heat through visco-thermal effects. Their acoustic performance, generally expressed in terms of sound absorption coefficients, depends on their micro-structural characteristics and is strongly influenced by their density. Even though various studies have shown that bio-based or recycled porous materials can achieve acoustic performance comparable to traditional solutions, many of these unconventional materials remain in a research or prototyping phase with limited commercial diffusion. While several studies have analysed the acoustic properties of different kinds of sustainable fibrous materials, there is a notable lack of comprehensive characterization of their physical properties and a systematic approach to design optimization to achieve acoustic performance comparable to traditional sound-absorbing materials.

This paper addresses this need by presenting a comprehensive methodology to develop and acoustically optimise sustainable fibrous materials, focusing on both bio-based and recycled alternatives. Such materials offer a promising pathway to significantly reduce the embodied carbon and operational energy of buildings, directly contributing to a circular economy in the construction sector and fostering a more sustainable urban future. Section 2 provides the theoretical framework and describes an inverse characterization approach suitable for a wide range of acoustic fibrous materials. Section 3 illustrates different case studies, demonstrating how the proposed methodology can be employed to develop sustainable sound-absorbing materials, including bio-based solutions that can achieve Class A acoustic performance like traditional materials, and to design mixtures of recycled fibres by predicting their acoustic performance. Finally, Section 4 discusses the key challenges for the real-world application and commercialization of bio-based sustainable fibrous panels.

This article, invited by the RIA editorial board following the oral presentation at the AIA International Symposium "Innovative Materials in Acoustics: Between Sustainability and Technology", does not present on a novel study. Instead, it is a comprehensive synthesis of several existing studies whose results were partially presented in various journals and at scientific conferences. To ensure consistency and coherence across all data, the findings from these studies have been thoroughly reanalysed and integrated using a single, unified methodology, which is described in the next section. All original sources are thoroughly referenced.

## 2 | Materials and methods

Optimizing the acoustic performance of porous materials necessitates the integration of experimental techniques and analytical models. This combined approach significantly reduces the time and cost associated with developing new materials. The following sections outline the various phases of the optimization process developed at the Acoustics Laboratory within the Department of Engineering at the University of Ferrara. While this discussion primarily focuses on fibrous materials, the methodology can be extended, with appropriate modifications, to include cellular materials (open-cell foams) and aggregates of recycled materials.

### 2.1 | Experimental characterisation

The first phase of experimental characterization aims to determine the acoustic descriptors and physical macrostructural properties (also defined transport parameters) of the fibrous material under analysis. This involves testing small material samples using laboratory equipment. The primary instrument used in this phase is the impedance tube (or plane wave tube), for measuring the surface acoustic impedance and normal incidence acoustic absorption. This technique, standardized by ISO 10534-2 [14], allows us to test very small quantities of material under controlled and well-known conditions, yielding acoustic information across a wide frequency range. For the specific equipment we use, samples have a 45 mm diameter, and measurements cover a frequency range from 100 Hz to 4300 Hz, as shown in Fig. 1. This initial experimental phase, especially for fibrous materials, can generally be applied to loose fibres, from which optimised panels will be made of a small quantity of loose fibres (approx. 10 grams) is progressively compressed inside the sample holder. This allows us to obtain a series of measurements at decreasing thickness and increasing density. This process it is very fast, does not require prototypes of samples at varying densities while can provide information about the acoustic behaviour of the materials as a function of density changes.

Besides impedance tube acoustic measurements, additional experimental tests can be performed on small samples to evaluate the transport parameters that influence the

acoustic performance of porous material, which require specialised experimental equipment. Examples include devices for measuring airflow resistivity $\sigma$ (ISO 9053-1 [15], or ISO 9053-2 [16]), porosity $\varphi$, tortuosity $\alpha_\infty$, viscous $\Lambda$ and thermal $\Lambda'$ characteristic lengths. While there aren't specific standards for porosity, tortuosity, and characteristic lengths, several methods are described in the literature (e.g., [17-24]). Moreover, indirect and inversion characterisation methods have been proposed by several authors [25-30]. Numerical approaches are also commonly used to characterise the transport parameters of a porous medium, by geometrically modelling its micro-structure in a Representative Volume Element (RVE) [31-34]. A comprehensive review of direct, indirect, and inverse measurement techniques used to assess the transport parameters of acoustic porous materials have been recently published by Di Giulio et al. [35]. Additionally, for fibrous materials, whose structure is relatively simple and changes predictably with compression, Santoni et al. [36] developed an optimization process that doesn't require these direct measurements. The transport parameters are determined as a function of the material density through an inversion method based on the measured normal incidence sound absorption coefficient. his method is further described in Section 2.2.

The final product validation requires the experimental characterization of its acoustic performance. Sound absorbing panels have to be tested by measuring samples with a surface area between 10 m$^2$ and 12 m$^2$ in a reverberation chamber (Fig. 2), according to the standard ISO 354 [37]. The experimental evaluation of the diffuse sound field absorption coefficient is essential for certifying the final product and the rate its acoustic performance according to the standard ISO 11654 [38]. The main limitation of this technique is that it requires a significant material surface area, which comes with associated production or prototyping costs. Furthermore, the diffuse sound field sound absorption coefficients results, measured according to this standard, strongly depend on the reverberation chamber's characteristics, especially for materials with high sound absorption. For these reasons, within the product optimization process, we aim to minimize the use of this technique, reserving it primarily for the final validation of the finished product and its acoustic certification.

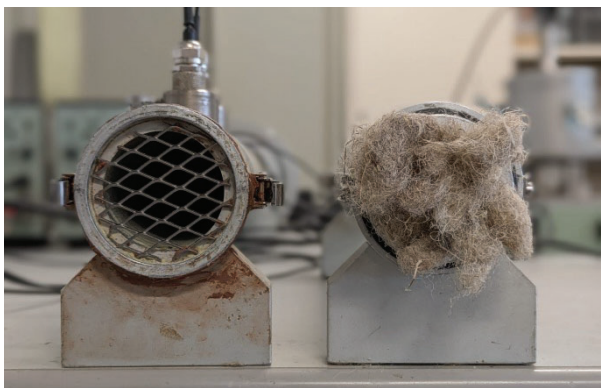

**Fig. 1 – Impedance tube test ring and fibrous material mounting**
***Tubo ad impedenza e montaggio del materiale fibroso***

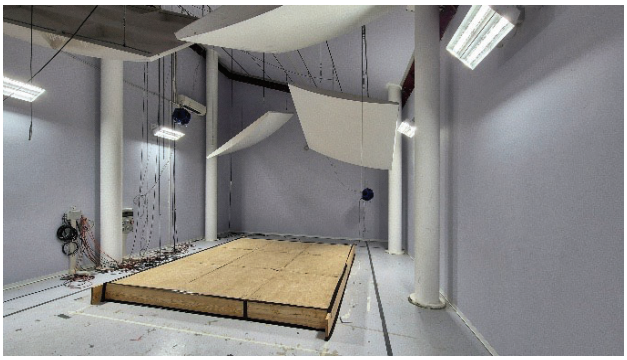

**Fig. 2 – Testing sample installed into the reverberant chamber**
***Camera riverberante con campione di prova installato***

## 2.2 | Acoustic analytical model

The analytical modelling of acoustic wave propagation in fibrous materials, as a first approximation, focuses on the viscous and thermal effects introduced by the material's structure, which is considered rigid and motionless. The material, comprising a fluid phase and a solid phase, is thus modelled as an equivalent dissipative fluid. Its acoustic properties are described by either the characteristic acoustic impedance ($Z_c$) and propagation constant ($k_c$), or by the effective density ($\rho_e$) and effective compressibility ($K_e$). These acoustic properties are expressed as functions of frequency ($f$), the parameters of the fluid saturating the material structure (air), and physical parameters that describe the material's structure and its viscous and thermal effects on acoustic wave propagation within the medium: the transport parameters.

There is extensive literature on analytical models for porous materials, primarily distinguished by the number of physical parameters required to describe the acoustic field within the medium. For fibrous materials, notable examples include the Delany-Bazley empirical model [39], which uses airflow resistivity as its sole parameter, and the Miki model [40] which adds porosity and tortuosity to the previous model. Semi-phenomenological multi-parametric models have also been proposed, such as the 5-parameter model based on the works of Johnson et al. [41] and of Champoux and Allard [42], known as the JCA model. This widely use method was further extend by Lafarge et al. [43] (JCAL, a 6-parameter model) and by Pride et al. [44] (JCAPL, a 8-parameter model). These multi-parametric models offer the advantage of better describing acoustic propagation in media with more complex structures (like foams or aggregates). They also effectively model the acoustic field in highly compacted fibrous materials (i.e., those with reduced porosity, $\varphi < 0.95$).

For the studies on sustainable fibrous materials, detailed in Section 3, it is preferable to use multi-parametric models like JCA. This is because the characteristic fibre dimension is often quite large, and to achieve high acoustic performance, these fibres must be significantly compressed, resulting in reduced porosities. Within the JCA framework, the frequency-dependent complex effective density $\rho_e$, which accounts

for inertial and viscous forces, is expressed by the following equation:

$$\rho_e = \frac{\alpha_\infty \rho_0}{\phi}\left[1 + \frac{\sigma\phi}{j\omega\alpha_\infty\rho_0}\sqrt{1 + j\frac{4\eta\alpha_\infty^2\rho_0\omega}{\sigma^2\Lambda^2\phi^2}}\right] \quad (1)$$

Simultaneously, the complex frequency-dependent dynamic bulk modulus $K_e$, which incorporates thermal exchanges between the material's frame and the fluid, is determined as:

$$K_e = \frac{\gamma P_0/\phi}{\gamma - (\gamma-1)\left[1 - j\frac{8\eta}{\rho_0\omega P_r \Lambda'^2}\sqrt{1 + \frac{j\rho_0\omega P_r\Lambda'^2}{16\eta}}\right]^{-1}} \quad (2)$$

In these equations, $\omega = 2\pi f$ is the angular frequency, $\rho_0$ represents the density of air, $\gamma$ is the heat capacity ratio, $P_r$ is the Prandtl number, $\eta$ is the dynamic viscosity of air, and $P_0$ is the ambient pressure.

From the complex effective density and dynamic bulk modulus given in Eqs. (1) and (2), we can compute the characteristic impedance $Z_c$ and the complex wavenumber $k_c$ of the equivalent fluid medium as follows:

$$Z_c = \sqrt{\rho_e K_e} \quad (3)$$

$$k_c = \omega\sqrt{\frac{\rho_e}{K_e}} \quad (4)$$

For a porous material of thickness $h$ placed on a rigid, reflecting boundary, the surface impedance for normal incidence ($Z_s$) is given by:

$$Z_s = -jZ_c\cot(k_c h) \quad (5)$$

Finally, the normal incidence sound absorption coefficient ($\alpha_n$) is evaluated as:

$$\alpha_n = \frac{4\mathrm{Re}\left\{\frac{Z_s}{\rho_0 c_0}\right\}}{\left|\frac{Z_s}{\rho_0 c_0}\right|^2 + 2\mathrm{Re}\left\{\frac{Z_s}{\rho_0 c_0}\right\} + 1} \quad (6)$$

Here, $c_0$ represents the speed of sound in air.

### 2.3 | Acoustic fibrous material optimisation

The inverse characterisation approach described in reference [36] can be applied to optimise the acoustic performance of fibrous materials. The transport parameters are expressed through a set of analytical equations. The open-cell porosity $\varphi$, is evaluated from the fibre's density $p_s$ and the apparent density of the material $\rho$ as:

$$\phi = 1 - \frac{\rho}{\rho_s} \quad (7)$$

The material's airflow resistivity $\sigma$ can be approximated as a function of porosity $\varphi$ and the effective radius $r_e$ of an equivalent 2D monodisperse fibrous medium [45,33]:

$$\sigma = \frac{\eta}{(2r_e)^2}\frac{\sqrt{1-(1-\phi)}}{0.21\left(\frac{0.71}{1-\phi} - 3\sqrt{\frac{0.71}{1-\phi}} + 3 - \sqrt{\frac{1-\phi}{0.71}}\right)} \quad (8)$$

The remaining transport parameters used in the JCA model can be expressed analytically as functions of porosity $\varphi$ or the effective radius $r_e$ The latter is one of the design parameters of the multi-variable function to be optimized. The high-frequency limit of tortuosity $\alpha_\infty$, is computed using Archie's empirical law based on the material's porosity $\varphi$ [46]:

$$\alpha_\infty = \left(\frac{1}{\phi}\right)^\beta = \left(\frac{1}{\phi}\right)^{0.9574} \quad (9)$$

Although the constant $\beta$ could be generally considered a variable depending on the microstructure of the fibrous medium, a constant value $\beta$ = 0.9574 was assumed, as proven to be suitable for a wide range of fibres independently of their effective radius $r_e$ [36]. The scale-of-pores geometrical quantities representing viscous $\Lambda$ and thermal $\Lambda$' characteristic lengths are determined using empirical equations proposed by Pompoli [13].

$$\Lambda = A_1 r_e(1-\phi)^{-A_2} \quad (10)$$

$$\Lambda' = A_3 r_e(1-\phi)^{-A_4} \quad (11)$$

The unknown coefficients, denoted as $A_i$ (with $i$ = 1,2,3,4) along with the effective radius $r_e$, serve as the optimization design variables to be determined by a minimization algorithm. This algorithm calculates the normal incidence sound absorption coefficient using the JCA model, with the transport parameters expressed through Eqs. (7) to (11). The primary goal of this optimization is to determine this set of design variables $x = \{r_e, A_1, A_2, A_3, A_4\}$, that minimizes an objective function, $F(x)$. This function is defined based on the normalised difference between the experimentally measured normal incidence sound absorption coefficients $\alpha_{n,exp}$ and those predicted by the JCA model $\alpha_{n,JCA}$, averaged over $m$ frequency lines and $n$ investigated densities.

$$\mathcal{F}(x) = \sum_{i=1}^{n}\frac{1}{n}\sum_{l=1}^{m}\frac{1}{m}\left|\alpha_{n,exp,i,l} - \alpha_{n,JCA,i,l}\right| \quad (12)$$

The minimisation of the objective function given in Eq. (12) defines the design variable $x$ and thus the transport parameters required as input data by the JCA model, expressed as a function of the material density.

Using the transport parameter density functions determined through this inverse characterization approach, we can predict the acoustic performance of porous materials. Through the Transfer Matrix Method (TMM) [47], the sound absorption coefficient can be evaluated whether the material is standalone or integrated within a multilayer system, such as with an air cavity or a screed layer. TMM is a widely used approach for investigating plane wave propagation in laterally infinite multilayer structures. These structures can encompass various media, including equivalent fluid, elastic, and poroe-

lastic materials, as well as porous or impervious screens and resonators. The TMM framework considers an acoustic plane wave incident at an angle $\theta$ on the system being investigated, with the system backed by a rigid, reflective wall termination. The sound absorption coefficient is then computed as:

$$\alpha(\theta) = 1 - \left| \frac{Z_s(\theta)\cos\theta - \rho_0 c_0}{Z_s(\theta)\cos\theta + \rho_0 c_0} \right|^2 \quad (13)$$

As expressed by Eq. (13), the surface impedance $Z_s$, thus the sound absorption coefficient $\alpha$, depend upon the angle of incidence $\theta$ of the impinging plane wave. The diffuse field sound absorption coefficient can be approximated as:

$$\alpha_d = \frac{\int_0^{\pi/2} \alpha(\theta)\cos\theta\sin\theta \mathrm{d}\theta}{\int_0^{\pi/2} \cos\theta\sin\theta \mathrm{d}\theta} \quad (14)$$

The TMM assumes laterally infinite media, leading to potential deviations when comparing predicted results with experimental sound absorption coefficients (measured according to ISO 354). However, the accuracy of the TMM approach can be improved by introducing the finite-size radiation impedance to airborne excitation $Z_R(\theta)$ [48–51] when computing the diffuse field incidence sound absorption coefficient:

$$\alpha_{d,f} = \frac{\int_0^{\pi/2} \frac{4\Re\{Z_s(\theta)\}}{|Z_s(\theta)+Z_R(\theta)|^2}\sin\theta \mathrm{d}\theta}{\int_0^{\pi/2} \cos\theta\sin\theta \mathrm{d}\theta} \quad (15)$$

## 3 | Optimisation examples

### 3.1 | Jute fibre

This study focused on developing two sound-absorbing panels made from jute fibre for indoor applications. The first is a 40 mm thick panel for wall-mounting applications, and the second is a thinner panel (20 mm) designed for false suspended ceilings with an air cavity. These panels were manufactured in India using jute fibres and natural latex as a binder.

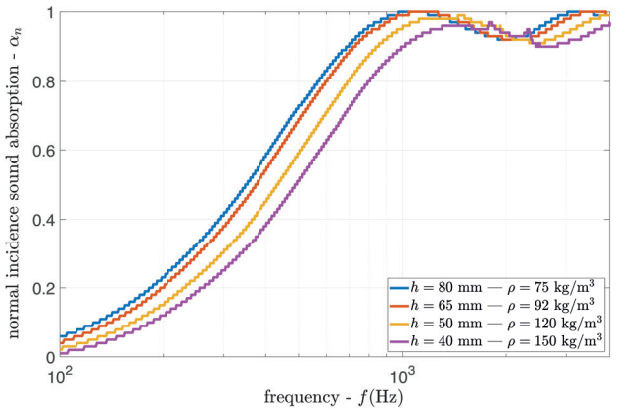


**Fig. 3 – Normal incidence sound absorption coefficient: experimental measurement on various combinations of thickness and density**

***Coefficiente di assorbimento acustico per incidenza normale: misure sperimentale su diverse combinazioni di spessore e densità***

Jute fibres are sourced from Corchorus Capsularis plants, a species of the Malvaceae family, abundant in the eastern monsoon regions. The production process, which utilizes natural latex as a binder, results in a 100% biodegradable panel. The acoustic design process for both panels started from the experimental characterisation of a small quantity of loose fibres. We used an impedance tube to measure the normal incidence sound absorption as the material was progressively compressed, as described in Section 2.1. The experimental results obtained for different combinations of density and thickness are shown in Fig. 3.

From the experimental results, we derived the transport parameters required by the JCA equivalent dissipative fluid model, expressed as density functions, using the inverse characterisation approach detailed in Section 2.3. Table 1 presents the calculated physical parameters for densities ranging from 120 to 240 kg/m$^3$.

**Tab. 1 – Transport parameters obtained from jute loose fibres as a function of the sample density though inversion characterization**

***Parametri di trasporto ricavati con metodo di inversione dalle misure sulle fibre sciolte di juta in funzione della densità***

| $\rho$ [kg/m$^3$] | $\varphi$ [–] | $\sigma$ [kNs/m$^4$] | $\alpha_\infty$ [–] | $\Lambda$ [μm] | $\Lambda'$ [μm] |
|---|---|---|---|---|---|
| 120 | 0.91 | 15.9 | 1.10 | 65 | 133 |
| 140 | 0.89 | 21.1 | 1.12 | 50 | 123 |
| 160 | 0.88 | 27.3 | 1.13 | 39 | 115 |
| 180 | 0.86 | 34.8 | 1.15 | 32 | 108 |
| 200 | 0.85 | 43.7 | 1.17 | 27 | 102 |
| 220 | 0.83 | 54.3 | 1.19 | 23 | 97 |
| 240 | 0.82 | 66.8 | 1.22 | 19 | 93 |

Using the TMM approach, including the diffuse field assumption and the finite-size correction proposed by Rhazi et al. [49] (as described in Section 2.3), we estimated the diffuse incidence sound absorption performance of the two systems, for various combinations of panel thickness, density (and optional air cavity). The estimation directly correlates with results experimentally obtainable in a reverberation chamber. The primary objective of this optimisation, requested by Hubbub ApS, was to develop the two systems capable of achieving Class A performance ($\alpha_w \geq 0.90$) according to ISO 11654. The entire optimization procedure was rigorously validated through experimental tests performed on 10.8 m$^2$ panels in a reverberation chamber in accordance with ISO 354. Table 2 presents the computed $\alpha_w$ values at different densities, for both analysed systems. The optimisation goal was to identify the optimal density that would enable the target acoustic performance ($\alpha_w \geq 0.90$), while meeting the client's specified panel thickness requirements (driven by commercial and production requirements).

As shown in Table 2, achieving Class A performance requires specific minimum densities for each panel configuration. For the 40 mm wall-mounted solution, a minimum density of 220 kg/m$^3$ is necessary. Conversely, the 20 mm panel

combined with a 200 mm air cavity demands a lower minimum density of 160 kg/m³.

**Tab. 2 – Predicted $\alpha_w$ as a function of the fibrous panel density in the wall-flush mounting and suspended ceiling configurations: jute fibres**

***Valori calcolati di $\alpha_w$ in funzione della densità dei pannelli per configurazione a parete e controsoffitto: fibre di juta***

| $\rho$ [kg/m³] | $\alpha_{w,40mm}$ (wall-panel) | $\rho$ [kg/m³] | $\alpha_{w,20/200mm}$ (false ceiling) |
|---|---|---|---|
| 160 | 0.80 | 120 | 0.80 |
| 180 | 0.85 | 140 | 0.85 |
| 200 | 0.85 | 160 | 0.90 |
| 220 | 0.90 | 180 | 0.90 |
| 240 | 0.90 | 200 | 0.90 |

Fig. 4 presents the computed diffuse incidence sound absorption coefficient in octave band spectra, for the 40 mm panel at different densities. This figure also details the $\alpha_w$ calculation reference curves (dotted black lines), specified in ISO 11652.

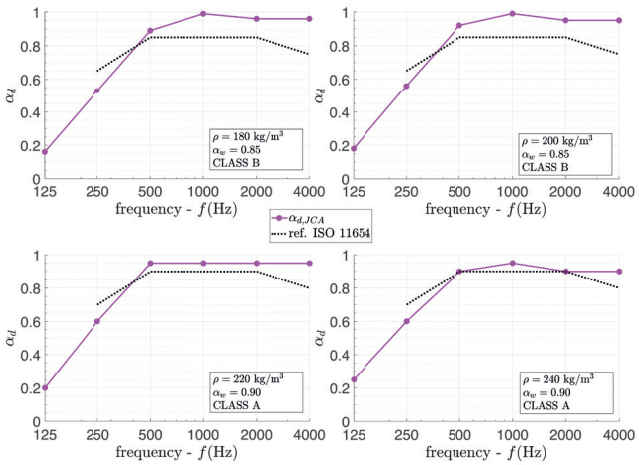


**Fig. 4 – Evaluation of $\alpha_w$ for wall-flush mounted 40 mm panels of different densities from the octave band sound absorption coefficient computed trough the analytical model.**

***Calcolo di $\alpha_w$ per pannelli di 40 mm di diverse densità dalle curve in bande di ottava del coefficiente di assorbimento acustico stimato con metodo analitico***

For the investigated systems, the weighted sound absorption coefficient $\alpha_w$ is primarily governed by the acoustic performance at frequencies below 250 Hz, as clearly illustrated in Fig. 4 for the 40 mm panel across various densities. Consequently, increasing the panel's density while keeping its thickness constant effectively enhances low-frequency absorption, allowing an $\alpha_w \geq 0.90$ value to be achieved. Based on these findings, we selected densities of 220 kg/m³ for the 40 mm wall-mounted solution and 160 kg/m³ for the 20 mm panel with a 200 mm air cavity in the suspended ceiling configuration.

Panels manufactured according to these specifications were subsequently tested in a reverberation chamber. Fig. 5 presents the experimental results for diffuse incidence sound absorption (in one-third octave bands), comparing them directly with the TMM calculated results. This comparison reveals a remarkable agreement between our computed results and the experimental sound absorption coefficient. Minor differences at high frequencies are attributed to the experimental approach outlined in ISO 354.

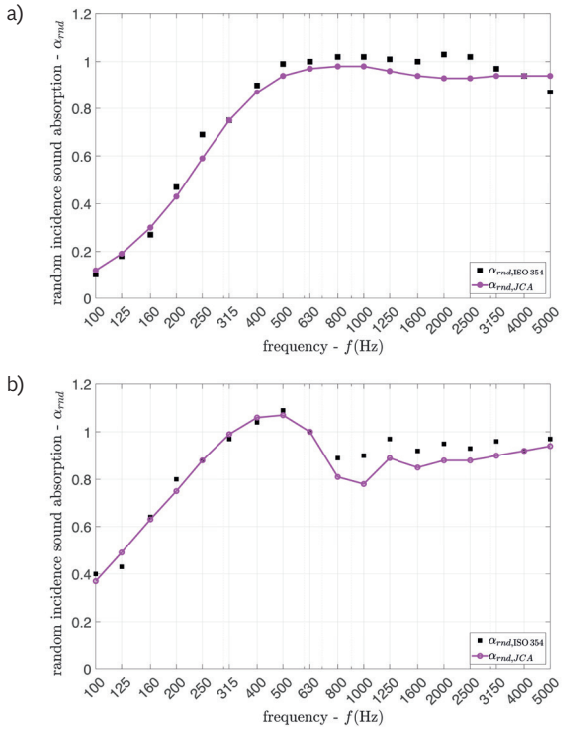


**Fig. 5 – Diffuse incidence sound transmission coefficient: comparison between experimental and predicted results – a) 40 mm panels (wall configuration, density 220 kg/m³); b) 20 mm panels with 200 mm air cavity (suspended ceiling configuration, density 160 kg/m³)**

***Coefficiente di assorbimento acustico per incidenza diffusa: confronto tra i risultati sperimentali e quelli previsionali – a) pannelli da 40 mm (soluzione a parete, densità 220 kg/m³); b) pannelli da 20 mm (con intercapedine da 200 mm, densità 160 kg/m³)***

## 3.2 | Posidonia fibre

This study on Posidonia fibres stems from the urgent need to find a sustainable use for a material currently classified as special waste, with disposal incurring significant costs for coastal municipalities. These materials, scientifically known as aegagropiles, appear as ellipsoidal agglomerations of fibres, shown in Fig. 6 (a). They are formed from the fraying leaves of Posidonia oceanica, which macerate in seawater until the fibres are released and then aggregated by wave action. Posidonia oceanica is an aquatic plant, endemic to the Mediterranean Sea, belonging to the Posidoniaceae family (monocotyledon angiosperms). It forms extensive meadows on sandy seabed near coastlines. This research [13] aimed to investigate the feasibility of using loose fibres obtained from Posidonia agglomerations to create sound-absorbing panels. To this end, we extracted loose fibres from the aegagropiles and evaluated their physical and acoustic characteristics across a range of densities (as described in Section 2.1). The Posidonia fibres investigated in this research were

collected from aegagropiles harvested on sandy beaches of Southern Sardinia. To ensure the removal of any residual moisture, they were left to sun-dry for several days. The fibres were manually separated from the aegagropiles, with any internal sand meticulously removed via sieving. Cylindrical samples, obtained from clean fibres were experimentally tested, as shown in Fig. 6 (b), measuring the normal incidence sound absorption coefficient, in accordance with the ISO 10534-2, by progressively compressing the sample to investigate a range of densities.


**Fig. 6 – Posidonia oceanica fibres: a) Aegagropiles deposited on the beach by the sea; b) Fibrous sample tested in the laboratory**

***Fibre di Posidonia oceanica: a) Egagropili depositate dal mare sulla spiaggia; b) campione fibroso testato in laboratorio***

The transport parameters required by the JCA model to analyse Posidonia fibres as a function of the material density were obtained from the experimental normal incidence sound absorption coefficient, as described in Section 2.3. Moreover, to further validate the inverse characterisation approach open porosity $\varphi$ and airflow resistivity $\sigma$ were experimentally measured, respectively according to the air volume compression method [17] and to the standard ISO 10534-2. The porosity was experimentally evaluated only for a given apparent density $\rho$ and then extended across the considered range using Eq. (7) by knowing the fibre density $\rho_s$ = 1518 kg/m$^3$. On the other hand, the airflow resistivity was measured for different densities obtained by progressively compressing the tested sample of loose fibres, to further validate the approach described in Section 2.3. The other physical parameters, namely the tortuosity $\alpha_\infty$ and the viscous and thermal characteristic lengths $\Lambda$ and $\Lambda'$ were obtained for each investigated density through a well-known inversion approach [29].

Fig. 7 presents a comparison of the density-dependent curves for the transport parameters evaluated using JCA modelling, alongside values obtained either experimentally or through other well-established inversion methodologies. In both cases, a good consistency among the different analysed methods is observed.

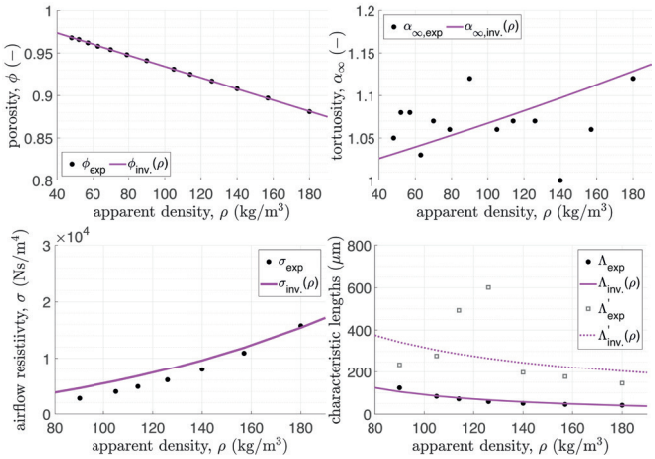


**Fig. 7 – Posidonia oceanica fibres: transport parameters used by the JCA model as a function of the material density**

***Fibre di Posidonia oceanica: parametri di trasporto del modello JCA al variare della densità del materiale.***

Fig. 8 further illustrates our findings by providing a comparison, in one-third octave bands, between experimental measurements of normal incidence acoustic absorption performed on samples at different compression ratios and results obtained from the JCA analytical model. Moreover, Table 3 compares the simulated weighted sound absorption coefficients $\alpha_W$ of Posidonia oceanica panels, with a thickness of 40 mm and 50 mm, at different densities. This comparison clearly demonstrates that Posidonia oceanica, a sustainable material, when compressed to an adequate density, can be effectively employed as a sound-absorbing material in its loose fibre form, offering acoustic performance able to reach a Class A rating comparable to traditional solutions.

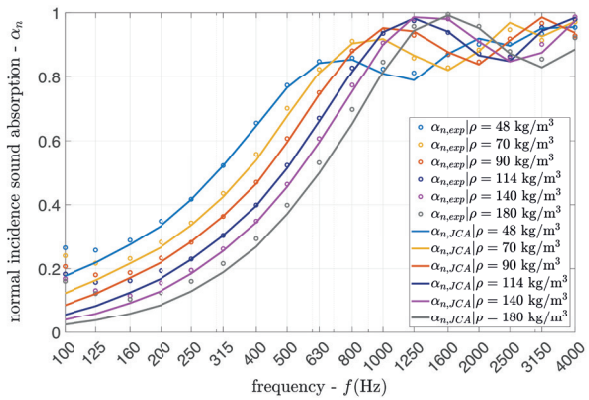


**Fig. 8 – Posidonia acoustic performance, comparison between predicted and experimental results**

***Prestazioni acustiche fibre di Posidonia, confronto tra dati previsionali e sperimentali***

**Tab. 3 – Predicted $\alpha_w$ as a function of the fibrous panel density computed from TMM predictions: Posidonia fibres**

***Valori calcolati di $\alpha_w$ in funzione della densità dei pannelli: valori calcolati con TMM: fibre di posidonia***

| $\rho$ [kg/m³] | 50 | 100 | 150 | 200 | 250 |
|---|---|---|---|---|---|
| $\alpha_{w,40mm}$ | 0.65 | 0.75 | 0.75 | 0.8 | 0.85 |
| Class | C | C | C | B | B |
| $\alpha_{w,50mm}$ | 0.70 | 0.85 | 0.90 | 0.95 | 1.00 |
| Class | C | B | A | A | A |

### 3.3 | Hemp fibre

Although several studies exist regarding the acoustic characterization of natural fibres, as detailed in the introduction of this paper, there is a notable lack of correlation with fibre type or geometry, and limited detail on the specific processing and chemical treatments involved in their production. This motivated a study investigating how different production processes can affect the acoustic properties of hemp fibres [11], ultimately aiming for their optimization. The experimental analysis was conducted on loose, binder-free hemp fibres (Cannabis Sativa var. 'Lipko') obtained through four consecutive processes: mechanical carding (1.CAR), alkaline treatment with NaOH (5% 1h) (2.NaOH), mechanical wide-tooth combing (3.WTC), mechanical fine-tooth combing (4.FTC). As an example, Fig. 9 shows Scanning Electron Microscope (SEM) images of the hemp fibres after different processing treatments.

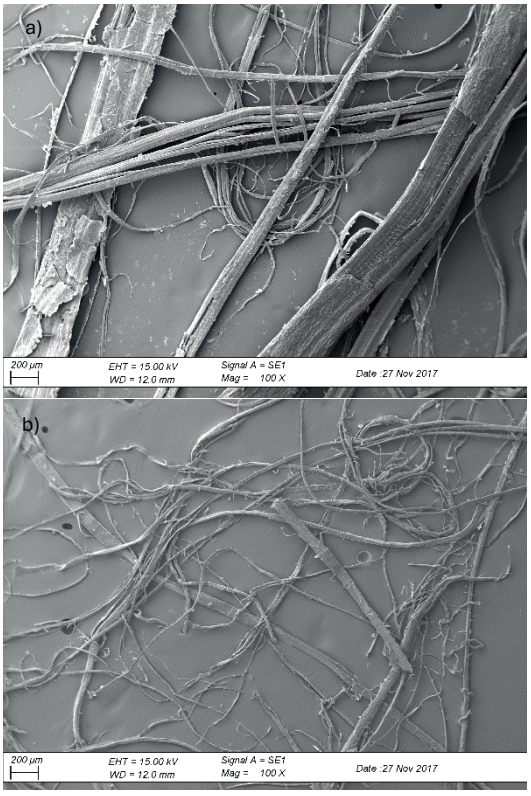


**Fig. 9 – SEM images of the hemp fibers at different processing stages: a) irst processing stage (1.CAR); b) Final processing stage (4.FTC)**

***Immagine al SEM delle fibre di canapa: a) primo processo di lavorazione (1.CAR); b) ultimo processo di lavorazione (4.FTC)***

While SEM images are typically used to determine fibre diameter distribution, natural fibres, like hemp, often show high variability, as demonstrated in Fig. 9. For this reason, an alternative approach to characterise the size of hemp fibres obtained after each process is through the effective radius $r_e$ introduced in Eq. (8). To this purpose, for each processing stage, we tested loose hemp fibres in an impedance tube to measure their normal incidence sound absorption. We did this by progressively increasing their compression ratios, following the methodology described in Section 2.1. Fig. 10 illustrates the normal incidence sound absorption coefficient as a function of the apparent density of the fibrous samples after the different processes. This shows that, regardless of the process, compressing the samples significantly influences the measured sound absorption. However, the acoustic performance also heavily depends on the fibre's characteristics, which are directly related to the specific treatment each material underwent. To highlight this, Fig. 11 compares the normal incidence sound transmission coefficients measured on samples from each process at the same density.

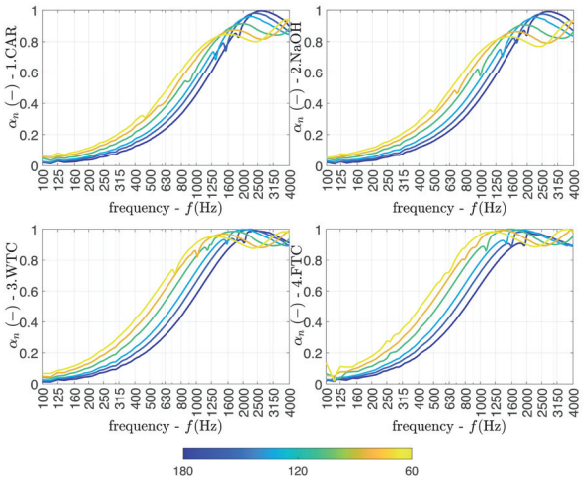


**Fig. 10 – Hemp acoustic performance: experimental normal incidence sound absorption coefficient after different processes as a function of the material density**

***Prestazioni acustiche fibre di Canapa: coefficiente di assorbimento acustico per incidenza normale misurato a varie densità dopo i diversi trattamenti***

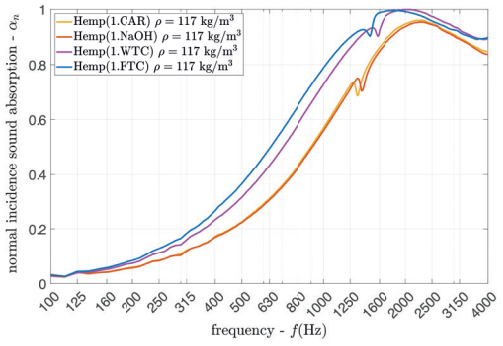


**Fig. 11 – Hemp acoustic performance: experimental normal incidence sound absorption coefficient after the different processes on samples with density 117 kg/m³**

***Prestazioni acustiche fibre di Canapa: coefficiente di assorbimento acustico per incidenza normale misurato dopo i diversi trattamenti su provini con densità apparente pari a 117 kg/m³***

Based on these experimental datasets, we estimated the transport parameters for each type of hemp fibre as a function of material density by applying the inverse characterization approach described in Section 2.3. As Fig. 12, illustrates, the physical parameters vary according to density consistently with our experimental sound absorption coefficient observations. Fig. 12 displays only the airflow resistivity and the viscous and thermal characteristic lengths. Porosity and tortuosity are not shown as they are not significantly influenced by the processing method; they primarily depend on fibre density and the sample's compression ratio, as expressed in Eqs. (7) and (9). It is noteworthy that the alkaline treatment (2.NaOH), which follows the carding process (1.CAR), has a limited influence on both acoustic performance and the physical parameters. Conversely, the mechanical combing treatments (both 3.WTC and 4.FTC) significantly improve the fibrous material's acoustic performance. This behaviour is consistently reflected in the physical parameters, showing an increase in airflow resistivity (due to a reduction in fibre diameter) and a corresponding reduction in the characteristic lengths. These density-dependent transport parameters, evaluated for different hemp fibre types, can be used to optimize panel density to meet specific acoustic requirements, as illustrated in Section 3.1.

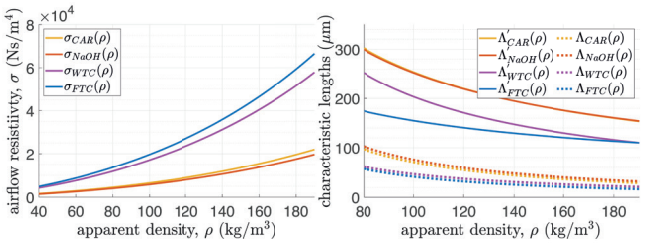


**Fig. 12 – Physical parameters obtained for Hemp fibres as a function of the density: a) airflow resistivity; b) viscous and thermal characteristic lengths**

***Parametri fisici ottenuti per le fibre di Canapa in funzione della densità: a) resistenza al flusso; b) lunghezze caratteristiche termica e viscosa***

Table 4 compares the computed weighted sound absorption coefficients $\alpha_w$ of 40 mm thick hemp fibre panels, at different densities, after each processing stage: 1.CAR, 2.NaOH, 3.WTC, and 4.FTC. This comparison clearly demonstrates that hemp fibres are a valuable alternative to traditional sound-absorbing materials, offering acoustic performance that can achieve a Class A rating when processed and compressed adequately.

**Tab. 4 – Predicted $\alpha_w$ as a function of the fibrous panel density computed from TMM predictions: hemp fibres**

***Valori calcolati di $\alpha_w$ in funzione della densità dei pannelli: valori calcolati con TMM: fibre di canapa***

| $\rho$ [kg/m³] | 50 | 100 | 150 | 200 |
|---|---|---|---|---|
| $\alpha_{W,40mm,1.CAR}$ | 0.65 | 0.75 | 0.75 | 0.80 |
| Class | C | C | C | B |
| $\alpha_{W,40mm,2.NaOH}$ | 0.65 | 0.75 | 0.75 | 0.80 |
| Class | C | C | C | B |
| $\alpha_{W,40mm,3.WTC}$ | 0.75 | 0.80 | 0.85 | 0.90 |
| Class | C | B | B | A |
| $\alpha_{W,40mm,4.FTC}$ | 0.75 | 0.80 | 0.90 | 0.90 |
| Class | C | B | A | A |

## 3.4 | Recycled fibre mixture

The automotive industry is increasingly using sound-absorbing components made from recycled fibre mixtures; a shift is driven by a need to cut costs and reduce the environmental footprint of vehicle production. These fibres often come from various industrial waste streams, such as recycled PET plastics or textile industry scraps. By varying percentages of coarser and finer fibres it is possible to optimise the acoustic and structural properties of the final component, tailored for specific applications. For instance, using larger diameter fibres results in stiffer components with enhanced load-bearing capacity. Conversely, incorporating finer fibres significantly improves the component's acoustic absorption performance. Typically, fibre mixtures are bound together by a specific type of fibre that, when heat-treated, undergoes localized fusion. This process creates mechanical connections between the fibres, forming a cohesive panel. The characteristics of each single type of fibre involved in the mixture and its percentage significantly affect the acoustic performance of the final product.

As presented in ref. [52], to accurately assess the acoustic properties of a fibre mixture from its composition and the characteristics of its loose constituent fibres, the equivalent density of the mixture ($\rho_{mix}$) is calculated as the weighted average of the density of each $i^{th}$ individual fibre type ($\rho_{f,i}$), based on its percentage by weight ($X_i$):

$$\rho_{mix} = \frac{1}{\sum_{i=1}^{n} \frac{X_i}{\rho_{f,i}}} \tag{16}$$

Similarly, an equivalent effective radius for the mixture $r_{e,mix}$ can be computed from the effective radius of each fibre type $r_{e,i}$ within the blend.

$$r_{e,\mathrm{mix}} = \sqrt{\frac{1}{\rho_{mix} \sum_{i=1}^{n} \frac{X_i}{\rho_{f,i} r_{e,i}^2}}} \tag{17}$$

From Eq. (7), the open porosity of the fibre mixture $\varphi_{mix}$ can be determined using its density ($\rho_s = \rho_{mix}$). The airflow resistivity of the fibre mixture $\sigma_{mix}$ depends on the mixture's effective radius $r_{e,mix}$ and its porosity $\varphi_{mix}$, as expressed in Eq. (8). The tortuosity $\alpha_{\infty,mix}$ only depends on the latter parameter, as given in Eq. (9). Consistently, equivalent values of the viscous and thermal characteristic lengths must be determined. While the most straightforward approach would suggest computing the arithmetic average of the values obtained for each fibre, this method has proven to be inaccurate. Therefore, the coefficients $A_{i,mix}$ required to determine the viscous characteristic

length $\Lambda_{mix}$ and thermal characteristics lengths $\Lambda'_{mix}$ of the mixture, given in Eqs. (10) and (11), are evaluated from the coefficients of the loose fibres involved in the mixture, considering their percentage weight $w_i$:

$$A_{i,\mathrm{mix}} = \frac{\sum_{i=1}^{n} w_i A_i}{\sum_{i=1}^{n} w_i} \tag{18}$$

As an example, the proposed methodology is applied to three different kind of fibres mixtures, taken from the work presented by Santoni et al. [52]. It should be noted that in the original work the loose fibres were modelled through the JCAL equivalent fluid model, and a different approach was adopted to characterise the required transport parameters, based on the experimental evaluation of the airflow resistivity at different compression ratios. The results presented in this paper, are obtained by characterising the loose fibres through the method described in Section 2 , based on the experimental normal incidence sound absorption coefficient measured at different compression ratios and the JCA equivalent fluid model. The three considered mixtures $m_a$, $m_b$, *and* $m_c$ are composed by six different recycled fibres which can be grouped in three different categories:

- PES (polyester) synthetic fibres, obtained from the made by recycling post-consumer plastic. PET (polyethylene terephthalate) is the most common polyester resin, primarily recycled from water bottles melted and re-extruded with different diameters. Loose fibres $lf_A$, $lf_B$ (PES) $lf_C$, $lf_D$ (PET).
- Cotton fibres (Cot), obtained from the mechanical recycling of textiles to be reused, coming from different supply chains (e.g., used clothing or industrial processes). In this case, the variability in the origin of the materials results in a wide variability in fibre size. Loose fibre $lf_E$.
- Bicomponent fibres (BiCo), used for the thermal bonding of fibres thanks to the presence of two coaxial layers of material with different melting points. When an intermediate temperature is reached during the thermal treatment of the mixture, the outer part of the fibre melts and bonds all the fibres together, providing mechanical stability to the component. Typically, this component can vary between 15% and 50%, depending on the mechanical properties desired for the panel. Loose fibre $lf_F$.

Table 5 provides the characteristics of the different loose fibres, including the nominal dtex (a commonly used unit expressing the fibre mass in grams per 10.000 meters of yarn),

**Tab. 5 – Loose fibres characteristics and mixtures composition**
***Caratteristiche delle fibre sciolte e composizione delle miscele***

| Loose fibre | | dtext | $\rho_f$ | $r_e$ | Fibre Mixture | | |
|---|---|---|---|---|---|---|---|
| Id | type | g/10km | kg/m³ | μm | $W_{m_a}$ | $W_{m_b}$ | $W_{m_c}$ |
| $lf_A$ | $PES_{11}$ | 1.1 | 1370 | 7 | – | 35% | – |
| $lf_B$ | $PES_{28}$ | 28.0 | 1370 | 35 | – | 10% | – |
| $lf_C$ | $PET_{15}$ | 1.5 | 1370 | 9 | 20% | – | – |
| $lf_D$ | $PET_{25}$ | 25.0 | 1370 | 37 | 30% | – | – |
| $lf_E$ | Cot | 2.0 | 1500 | 12 | 5% | 35% | 83% |
| $lf_F$ | BiCo | 4.4 | 1370 | 16 | 45% | 20% | 17% |

the density $\rho_f$ provided by the producer, and the effective radius $r_e$ determined through the inversion characterisation approach described in Section 2.

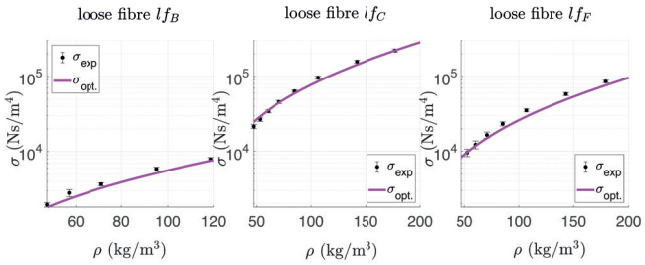


**Fig. 13 – Comparison between experimental airflow resistivity measured on loose fibre at different density and the optimised density-function computed from Eq. (8)**
***Confronto tra la resistività al flusso sperimentale misurata su fibre sciolte a diverse densità e la curva funzione della densità calcolata con l'Eq. (8)***

To evaluate the accuracy of this approach in characterizing these kinds of fibres, Fig. 13 compares the airflow resistivity density-function, computed according to Eq. (8), with the experimental results measured according to the standard ISO 9053-2 [16]. The experimental results, provided with error bars representing the associated standard deviation, were averaged over ten measurements at different compression rates. A generally good agreement can be observed between the experimental airflow resistivity values and the analytical curves. The slight underestimation of the airflow resistivity obtained from the analytical model can be associated with an overestimate of the effective radius due to the model's assumptions.

Additionally, Fig. 14 compares the experimental normal incidence sound absorption coefficient with the analytical results computed with the JCA model for different densities.

This comparison highlights a good approximation of the experimental results even though the investigated loose fibre samples exhibited a resonance that cannot be accounted for by the JCA model. To overcome this issue, the frequency range affected by the resonance was excluded from the optimization used to evaluate the fibres' transport parameters.

Finally, in Fig. 15 the experimental normal incidence sound absorption coefficients of three different fibre mixtures are compared to the analytical results computed using the JCA equivalent fluid model. The transport parameters used as input data in the JCA model are estimated from the parameters associated with the loose fibres employed in the mixture, as expressed in Eqs. (16) to (18). The results are plotted as a shaded area, representing the uncertainty associated with either the experimental measurements or the analytical results, related to the variation in sample density and thickness. A good approximation can generally be achieved by the adopted model, although it should be noted that accuracy decreases at higher densities, where the computed sound absorption slightly underestimates the experimental values. Nevertheless, this approach might represent a handy tool to design fibre mixtures, even in the automotive industry, where recycled

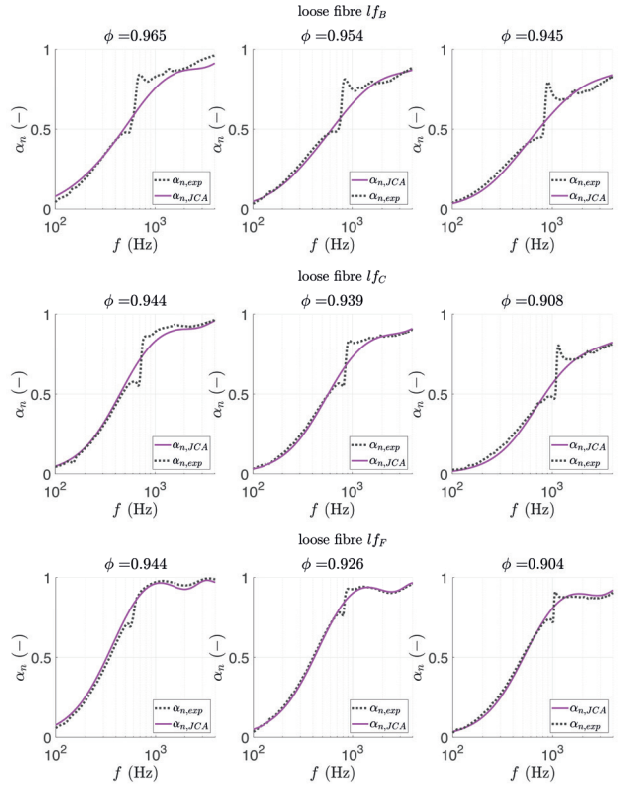


**Fig. 14 – Comparison between experimental and analytical normal incidence sound absorption coefficient for different types of recycled loose fibres at various densities**

***Confronto tra il coefficiente di assorbimento acustico per incidenza normale sperimentale e calcolato analiticamente per diversi tipi di fibre sciolte riciclate a varie densità***

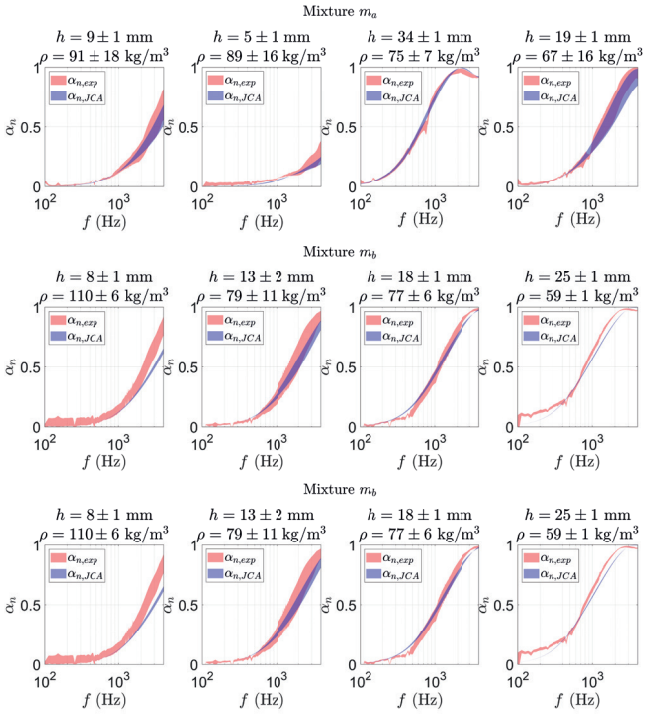


**Fig. 15 – Comparison between experimental and analytical normal incidence sound absorption coefficient for different mixtures of recycled fibres at various densities**

***Confronto tra il coefficiente di assorbimento acustico per incidenza normale sperimentale e calcolato analiticamente per diverse miscele di fibre riciclate a varie densità***

fibres are generally employed in fibre mixtures for acoustic treatments at high compression ratios. Although predictions might slightly underestimate the mixture's sound-absorbing performance, they predict the trend of the sound absorption coefficient with satisfying accuracy, as demonstrated by the results provided in Fig. 15.

## 3.5 | Discussion

Table 6 summarises and compares the acoustic properties of the different presented fibres, providing the key characteristics, such as fibre density, effective radius, and optimized coefficients for seven distinct fibres.

**Tab. 6 – Density, effective radius and optimised coefficients of different types of sustainable fibres**

***Densità, raggio effettivo e coefficienti ottenuti dall'ottimizzazione per diverse tipologie di fibre sostenibili***

| *Fibre* | $\rho_f$ kg/m$^3$ | $r_e$ μm | $A_1$ | $A_2$ | $A_3$ | $A_4$ |
|---|---|---|---|---|---|---|
| Jute | 1300 | 26.2 | 0.039 | 1.739 | 1.481 | 0.518 |
| Posidonia | 1518 | 33.6 | 0.065 | 1.372 | 1.209 | 0.755 |
| $Hemp_{FTC}$ | 1300 | 20.1 | 0.050 | 1.449 | 1.965 | 0.533 |
| $PES_{28}$ | 1370 | 34.9 | 0.274 | 0.993 | 0.630 | 0.919 |
| $PET_{15}$ | 1370 | 9.4 | 0.252 | 0.963 | 1.484 | 0.459 |
| Cot | 1500 | 12.0 | 0.237 | 0.995 | 0.418 | 0.839 |
| BiCo | 1370 | 16.2 | 0.212 | 0.993 | 1.937 | 0.469 |

To better illustrate the effect of these physical characteristics on transport parameters, the airflow resistivity density functions for the seven fibres are compared in Fig. 16. This comparison reveals that synthetic and textile fibres (i.e., $PET_{15}$, Cot, and BiCo) generally have a higher airflow resistivity than natural fibres (e.g., Posidonia and Jute) at a given density, due to their smaller radii. However, there are some exceptions. When synthetic fibres are designed with a larger diameter (i.e., $PES_{28}$), their airflow resistivity becomes comparable to that of natural fibres. Furthermore, while the dimensions of natural

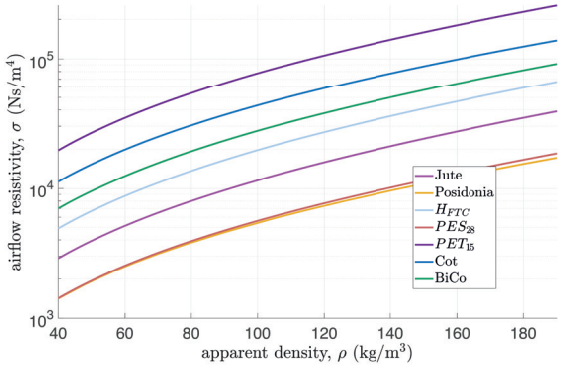


**Fig. 16 – Density-dependent airflow resistivity evaluated for different kind of fibres**

***Resistività al flusso determinata in funzione della densità per diverse tipologie di fibre***

fibres cannot be precisely designed, their acoustic properties can be optimized through specific manufacturing processes, as demonstrated by the $Hemp_{CAR}$ sample, which achieved an airflow resistivity similar to traditional fibrous materials after various treatments.

It is important to note that a higher airflow resistivity does not always translate to better acoustic performance. On the contrary, an excessive increase in material resistivity can lead to a reduction in sound absorption. Therefore, optimal acoustic performance can be achieved with materials having coarser fibres by adjusting their apparent density to modify the transport parameters.

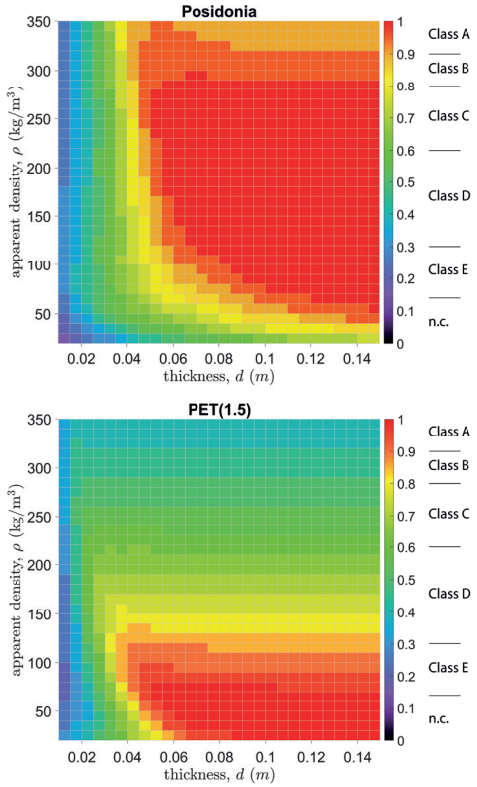


**Fig. 17 – Heat map represent the weighted sound absorption coefficient calculated as a function of the density and the thickness for two kinds of fibres: a) Posidonia; b) $PET_{15}$**

***Grafico a mappa di calore che rappresenta il coefficiente di assorbimento acustico ponderato calcolato in funzione della densità e dello spessore per due diverse fibre: a) Posidonia; b) $PET_{15}$***

This optimization process is graphically illustrated in Fig. 17, which compares the heat maps of the weighted sound absorption coefficient ($\alpha_w$) computed as a function of the density and the thickness for Posidonia and $PET_{15}$ fibres. This comparison clearly shows that both materials can achieve a Class A sound absorption rating with an adequate combination of thickness and apparent density. While the finer $PET_{15}$ fibres, can achieve a performance $\alpha_w \geq 0.9$ at lower density, they are less suitable for denser panels. In contrast, natural fibres like Posidonia exhibit better performance in denser panels. The graphs in Fig. 17 serve as a useful tool for quickly optimizing the density of sound-absorbing panels for a specific material and thickness.

## 4 | Applicability considerations

This final section discusses the practical applicability of sustainable fibrous sound-absorbing panels in real-world scenarios. While previous sections have demonstrated that these materials can be engineered to match the acoustic performance of traditional products, their market viability is contingent upon meeting stringent certification requirements. Key among these are fire safety, durability, and low chemical emissions.

A primary challenge is the inherent combustibility of untreated natural fibres. Achieving the necessary fire safety classifications, such as those defined by EN 13501-1 standard [53], requires the integration of fire-retardant treatments. However, common retardants, including halogenated, phosphorus-based, or inorganic compounds, are often synthetic chemicals that pose significant health and environmental risks. Their addition can also alter the fibre's porous structure, potentially affecting acoustic performance, and fundamentally compromise the material's end-of-life advantages by hindering biodegradability and complicating recycling. Nevertheless, industrial and academic research is very active in study solutions to overcome these issues, guaranteeing fire safety without undermining sustainability and acoustic performance of bio-based fibrous materials.

Furthermore, the long-term durability of bio-based panels must be ensured. They are susceptible to degradation from moisture, fungi, and microorganisms, often necessitating additional protective treatments. As mandated by certifications like the CE marking, products must be assessed not only for durability but also for their impact on indoor air quality, particularly the emission of Volatile Organic Compounds (VOCs). Ultimately, the successful commercialisation of sustainable acoustic solutions demands a holistic engineering approach that balances acoustic efficacy with these essential safety, health, and durability standards.

## 5 | Conclusions

This study successfully demonstrated the effectiveness and efficiency of a combined experimental and analytical methodology for optimizing the acoustic performance of sustainable fibrous materials. By integrating impedance tube measurements on a small amount of loose fibres with an inverse characterisation approach based on the JCA equivalent fluid model, we developed an easily implementable tool that significantly reduces the effort required to characterize the physical properties of fibrous materials.

Four case studies, involving different fibrous materials — jute, posidonia oceanica, hemp, and recycled fibre mixtures — are presented to illustrate the potential of this approach and assess its accuracy and reliability, even when applied to natural or recycled fibres. The results consistently showed that the approach provides a satisfyingly accurate prediction of a material's acoustic behaviour. For jute and hemp fibres, the optimization process successfully identified the ideal den-

sities and processing methods needed to achieve a Class A sound absorption rating, showcasing these sustainable materials as viable alternatives to traditional solutions. Specifically, the study revealed that mechanical combing significantly improves hemp fibre performance. Similarly, the research on posidonia oceanica proved that this material, currently classified as special waste, can be repurposed into an effective and sustainable sound-absorbing product. Finally, the analysis of recycled fibre mixtures demonstrated that the methodology could serve as a valuable design tool for accurately predicting the acoustic properties of complex fibre blends, widely used in the automotive industry, from the knowledge of the physical parameters of their individual components.

This research provides a practical and efficient tool for advancing the use of sustainable materials, fostering a more circular economy. While the model generally provides a good approximation of experimental results, a slight underestimation of sound absorption was noted at higher densities. Future work should focus on further extending the methodology by including a poro-elastic model, ensuring greater accuracy for a wider range of fibrous materials and densities.

## Conclusioni

Questo studio ha dimostrato con successo l'efficacia e l'efficienza di una metodologia ibrida, sperimentale e analitica, per l'ottimizzazione delle prestazioni acustiche di materiali fibrosi sostenibili. Integrando le misurazioni nel tubo a impedenza su una piccola quantità di fibre sciolte con un approccio di caratterizzazione inversa basato sul modello a fluido equivalente JCA, abbiamo sviluppato uno strumento di facile implementazione che riduce significativamente lo sforzo richiesto per caratterizzare le proprietà fisiche dei materiali fibrosi.

Vengono presentati quattro casi di studio, che coinvolgono diversi materiali fibrosi –iuta, posidonia oceanica, canapa e miscele di fibre riciclate – per illustrare il potenziale di questo approccio e valutarne l'accuratezza e l'affidabilità, anche se applicato a fibre naturali o riciclate. I risultati hanno mostrato che l'approccio fornisce una previsione sufficientemente accurata del comportamento acustico di un materiale. Per le fibre di iuta e canapa, il processo di ottimizzazione ha identificato con successo le densità ideali e i metodi di lavorazione necessari per raggiungere un coefficiente di assorbimento acustico di Classe A, dimostrando che questi materiali sostenibili sono valide alternative alle soluzioni tradizionali. Nello specifico, lo studio ha rivelato che il processo di pettinatura meccanica migliora significativamente le prestazioni delle fibre di canapa. Allo stesso modo, la ricerca sulla posidonia oceanica ha dimostrato che questo materiale, attualmente classificato come rifiuto speciale, può essere riutilizzato in un prodotto fonoassorbente efficace e sostenibile. Infine, l'analisi delle miscele di fibre riciclate ha evidenziato che la metodologia può essere impiegata come strumento di progettazione per prevedere le proprietà acustiche di miscele di fibre complesse, ampiamente utilizzate nell'industria automobilistica, partendo dalla conoscenza dei parametri fisici dei loro singoli componenti.

Questa ricerca fornisce uno strumento pratico ed efficiente per promuovere l'uso di materiali sostenibili, favorendo l'economia più circolare. Sebbene il modello fornisca generalmente una buona approssimazione dei risultati sperimentali, è stata notata una leggera sottostima dell'assorbimento acustico nei materiali a densità più elevate. Lo sviluppo futuro dovrebbe concentrarsi sull'ulteriore estensione della metodologia includendo un modello poro-elastico, garantendo una maggiore precisione per una più ampia gamma di materiali fibrosi e densità considerate.

## Bibliography


[1] F. Asdrubali, S. Schiavoni, K.V. Horoshenkov, A Review of Sustainable Materials for Acoustic Applications, Building Acoustics 19 (2012) 283–311. https://doi.org/10.1260/1351-010X.19.4.283.

[2] F. Asdrubali, F. D'Alessandro, S. Schiavoni, A review of unconventional sustainable building insulation materials, Sustainable Materials and Technologies 4 (2015) 1–17. https://doi.org/10.1016/j.susmat.2015.05.002.

[3] J. Zach, J. Hroudová, A. Korjenic, Environmentally efficient thermal and acoustic insulation based on natural and waste fibers: Environmentally efficient insulations based on natural and waste fibers, J. Chem. Technol. Biotechnol. 91 (2016) 2156–2161. https://doi.org/10.1002/jctb.4940.

[4] D. Kumar, M. Alam, P.X.W. Zou, J.G. Sanjayan, R.A. Memon, Comparative analysis of building insulation material properties and performance, Renewable and Sustainable Energy Reviews 131 (2020) 110038. https://doi.org/10.1016/j.rser.2020.110038.

[5] S. Islam, G. Bhat, Environmentally-friendly thermal and acoustic insulation materials from recycled textiles, Journal of Environmental Management 251 (2019) 109536. https://doi.org/10.1016/j.jenvman.2019.109536.

[6] F. Ye, H. Wei, Y. Xiao, U. Berardi, G. Quaranta, C. Demartino, Bio-based insulation materials in sustainable constructions: A review of environmental, thermal and acoustic insulation, durability, and mechanical performances, Renewable and Sustainable Energy Reviews 223 (2025) 115872. https://doi.org/10.1016/j.rser.2025.115872.

[7] P. Glé, E. Gourdon, L. Arnaud, Acoustical properties of materials made of vegetable particles with several scales of porosity, Applied Acoustics 72 (2011) 249–259. https://doi.org/10.1016/j.apacoust.2010.11.003.

[8] U. Berardi, G. Iannace, Acoustic characterization of natural fibers for sound absorption applications, Building and Environment 94 (2015) 840–852. https://doi.org/10.1016/j.buildenv.2015.05.029.

[9] K.H. Or, A. Putra, M.Z. Selamat, Oil palm empty fruit bunch fibres as sustainable acoustic absorber, Applied Acoustics 119 (2017) 9–16. https://doi.org/10.1016/j.apacoust.2016.12.002.

[10] A. Putra, K.H. Or, M.Z. Selamat, M.J.M. Nor, M.H. Hassan, I. Prasetiyo, Sound absorption of extracted pineapple-leaf fibres, Applied Acoustics 136 (2018) 9–15. https://doi.org/10.1016/j.apacoust.2018.01.029.

[11] A. Santoni, P. Bonfiglio, P. Fausti, C. Marescotti, V. Mazzanti, F. Mollica, F. Pompoli, Improving the sound absorption performance of sustainable thermal insulation materials: Natural hemp fibres, Applied Acoustics 150 (2019) 279–289. https://doi.org/10.1016/j.apacoust.2019.02.022.

[12] P. Soltani, E. Taban, M. Faridan, S.E. Samaei, S. Amininasab, Experimental and computational investigation of sound absorption performance of sustainable porous material: Yucca Gloriosa fiber, Applied Acoustics 157 (2020) 106999. https://doi.org/10.1016/j.apacoust.2019.106999.

[13] F. Pompoli, Acoustical Characterization and Modeling of Sustainable Posidonia Fibers, Applied Sciences 13 (2023) 4562. https://doi.org/10.3390/app13074562.

[14] ISO 10534-2: Acoustics — Determination of acoustic properties in impedance tubes Part 2: Two-microphone technique for normal sound absorption coefficient and normal surface impedance, (2023).

[15] ISO 9053-1: Acoustics — Determination of airflow resistance Part 1: Static airflow method, (2018).

[16] ISO 9053-2: Acoustics — Determination of airflow resistance. Part 2: Alternating airflow method, (2020).

[17] Y. Champoux, M.R. Stinson, G.A. Daigle, Air-based system for the measurement of porosity, The Journal of the Acoustical Society of America 89 (1991) 910–916. https://doi.org/10.1121/1.1894653.

[18] P. Leclaire, O. Umnova, K.V. Horoshenkov, L. Maillet, Porosity measurement by comparison of air volumes, Review of Scientific Instruments 74 (2003) 1366–1370. https://doi.org/10.1063/1.1542666.

[19] Y. Salissou, R. Panneton, Pressure/mass method to measure open porosity of porous solids, Journal of Applied Physics 101 (2007) 124913. https://doi.org/10.1063/1.2749486.

[20] R.J.S. Brown, Connection between formation factor for electrical resistivity and fluid – solid coupling factor in Biot's equations for acoustic waves in fluid – filled porous media, GEOPHYSICS 45 (1980) 1269–1275. https://doi.org/10.1190/1.1441123.

[21] D.L. Johnson, T.J. Plona, C. Scala, F. Pasierb, H. Kojima, Tortuosity and Acoustic Slow Waves, Phys. Rev. Lett. 49 (1982) 1840–1844. https://doi.org/10.1103/PhysRevLett.49.1840.

[22] J.F. Allard, B. Castagnede, M. Henry, W. Lauriks, Evaluation of tortuosity in acoustic porous materials saturated by air, Review of Scientific Instruments 65 (1994) 754–755. https://doi.org/10.1063/1.1145097.

[23] Ph. Leclaire, L. Kelders, W. Lauriks, M. Melon, N. Brown, B. Castagnède, Determination of the viscous and thermal characteristic lengths of plastic foams by ultrasonic measurements in helium and air, Journal of Applied Physics 80 (1996) 2009–2012. https://doi.org/10.1063/1.363817.

[24] Z.E.A. Fellah, S. Berger, W. Lauriks, C. Depollier, C. Aristégui, J.-Y. Chapelon, Measuring the porosity and the tortuosity of porous materials via reflected waves at oblique incidence, The Journal of the Acoustical Society of America 113 (2003) 2424–2433. https://doi.org/10.1121/1.1567275.

[25] O. Umnova, K. Attenborough, H.-C. Shin, A. Cummings, Deduction of tortuosity and porosity from acoustic reflection and transmission measurements on thick samples of rigid-porous materials, Applied Acoustics 66 (2005) 607–624. https://doi.org/10.1016/j.apacoust.2004.02.005.

[26] R. Panneton, X. Olny, Acoustical determination of the parameters governing viscous dissipation in porous media, The Journal of the Acoustical Society of America 119 (2006) 2027–2040. https://doi.org/10.1121/1.2169923.

[27] X. Olny, R. Panneton, Acoustical determination of the parameters governing thermal dissipation in porous media, The Journal of the Acoustical Society of America 123 (2008) 814–824. https://doi.org/10.1121/1.2828066.

[28] J.-P. Groby, E. Ogam, L. De Ryck, N. Sebaa, W. Lauriks, Analytical method for the ultrasonic characterization of homogeneous rigid porous materials from transmitted and reflected coefficients, The Journal of the Acoustical Society of America 127 (2010) 764–772. https://doi.org/10.1121/1.3283043.

[29] P. Bonfiglio, F. Pompoli, Inversion Problems for Determining Physical Parameters of Porous Materials: Overview and Comparison Between Different Methods, Acta Acustica United with Acustica 99 (2013) 341–351. https://doi.org/10.3813/AAA.918616.

[30] L. Jaouen, E. Gourdon, P. Glé, Estimation of all six parameters of Johnson-Champoux-Allard-Lafarge model for acoustical porous materials from impedance tube measurements, The Journal of the Acoustical Society of America 148 (2020) 1998–2005. https://doi.org/10.1121/10.0002162.

[31] F. Chevillotte, C. Perrot, R. Panneton, Microstructure based model for sound absorption predictions of perforated closed-cell metallic foams, The Journal of the Acoustical Society of America 128 (2010) 1766–1776. https://doi.org/10.1121/1.3473696.

[32] M. He, C. Perrot, J. Guilleminot, P. Leroy, G. Jacqus, Multiscale prediction of acoustic properties for glass wools: Computational study and experimental validation, The Journal of the Acoustical Society of America 143 (2018) 3283–3299. https://doi.org/10.1121/1.5040479.

[33] F. Pompoli, P. Bonfiglio, Definition of analytical models of non-acoustical parameters for randomly-assembled symmetric and asymmetric radii distribution in parallel fiber structures, Applied Acoustics 159 (2020) 107091. https://doi.org/10.1016/j.apacoust.2019.107091.

[34] T.G. Zieliński, R. Venegas, C. Perrot, M. Červenka, F. Chevillotte, K. Attenborough, Benchmarks for microstructure-based modelling of sound absorbing rigid-frame porous media, Journal of Sound and Vibration 483 (2020) 115441. https://doi.org/10.1016/j.jsv.2020.115441.

[35] E. Di Giulio, C. Perrot, R. Dragonetti, Transport parameters for sound propagation in air saturated motionless porous materials: A review, International Journal of Heat and Fluid Flow 108 (2024) 109426. https://doi.org/10.1016/j.ijheatfluidflow.2024.109426.

[36] A. Santoni, F. Pompoli, C. Marescotti, P. Fausti, Characterization of fibrous media transport parameters from multi-compression-ratio measurements of normal incidence sound absorption, The Journal of the Acoustical Society of America 157 (2025) 1185–1201. https://doi.org/10.1121/10.0035847.

[37] ISO 354: Acoustics — Measurement of sound absorption in a reverberation room, (2003).

[38] ISO 11654: Acoustics — Sound absorbers for use in buildings — Rating of sound absorption, (1997).

[39] M.E. Delany, E.N. Bazley, Acoustical properties of fibrous absorbent materials, Applied Acoustics 3 (1970) 105–116. https://doi.org/10.1016/0003-682X(70)90031-9.

[40] Y. Miki, Acoustical properties of porous materials. Modifications of Delany-Bazley models., J. Acoust. Soc. Jpn. (E), J Acoust Soc Jpn E 11 (1990) 19–24. https://doi.org/10.1250/ast.11.19.

[41] D.L. Johnson, J. Koplik, R. Dashen, Theory of dynamic permeability and tortuosity in fluid-saturated porous media, J. Fluid Mech. 176 (1987) 379–402. https://doi.org/10.1017/S0022112087000727.

[42] Y. Champoux, J.-F. Allard, Dynamic tortuosity and bulk modulus in air-saturated porous media, Journal of Applied Physics 70 (1991) 1975–1979. https://doi.org/10.1063/1.349482.

[43] D. Lafarge, P. Lemarinier, J.F. Allard, V. Tarnow, Dynamic compressibility of air in porous structures at audible frequencies, The Journal of the Acoustical Society of America 102 (1997) 1995–2006. https://doi.org/10.1121/1.419690.

[44] S.R. Pride, F.D. Morgan, A.F. Gangi, Drag forces of porous-medium acoustics, Phys. Rev. B 47 (1993) 4964–4978. https://doi.org/10.1103/PhysRevB.47.4964.

[45] A. Tamayol, M. Bahrami, Transverse permeability of fibrous porous media, Phys. Rev. E 83 (2011) 046314. https://doi.org/10.1103/PhysRevE.83.046314.

[46] G.E. Archie, The Electrical Resistivity Log as an Aid in Determining Some Reservoir Characteristics, Transactions of the AIME 146 (1942) 54–62. https://doi.org/10.2118/942054-G.

[47] J.-F. Allard, N. Atalla, Propagation of sound in porous media: modelling sound absorbing materials, 2nd ed, Wiley, Hoboken, N.J, 2009.

[48] M. Villot, C. Guigou, L. Gagliardini, Predicting the acoustical radiation of finite size multi-layered structures by applying spatial windowing on infinite structures, Journal of Sound and Vibration 245 (2001) 433–455. https://doi.org/10.1006/jsvi.2001.3592.

[49] D. Rhazi, N. Atalla, A simple method to account for size effects in the transfer matrix method, The Journal of the Acoustical Society of America 127 (2010) EL30–EL36. https://doi.org/10.1121/1.3280237.

[50] P. Bonfiglio, F. Pompoli, R. Lionti, A reduced-order integral formulation to account for the finite size effect of isotropic square panels using the transfer matrix method, The Journal of the Acoustical Society of America 139 (2016) 1773–1783. https://doi.org/10.1121/1.4945717.

[51] A. Santoni, P. Bonfiglio, P. Fausti, F. Pompoli, Computation of the Alpha Cabin Sound Absorption Coefficient by Using the Finite Transfer Matrix Method (FTMM): Inter-Laboratory Test on Porous Media, Journal of Vibration and Acoustics 143 (2021). https://doi.org/10.1115/1.4048395.

[52] A. Santoni, P. Bonfiglio, A. Magnani, C. Marescotti, F. Pompoli, P. Fausti, A hybrid approach for modelling the acoustic properties of recycled fibre mixtures for automotive applications, Applied Acoustics 182 (2021) 108272. https://doi.org/10.1016/j.apacoust.2021.108272.

[53] EN 13501-1 Fire classification of construction products and building elements – Part 1: Classification using data from reaction to fire tests, (2018).